Application of Deformable Models in Orthopaedic Surgery Planning*

J. M. Pardo[1], F. Vilariño[1], M. J. Carreira[1], R. Turnes[1], D. Cabello[1], J. Heras[2] and J. Couceiro[2]

[1] Dpto. Electrónica e Computación, Facultade de Física
[2]Servicio de Ciruxía Ortopédica, Complexo Hospitalario Universitario
Universidade de Santiago de Compostela, Spain

Total knee replacement (TKR) is a surgical procedure used by orthopaedic surgeons. It requires an adequate preoperative planning. Several parameters involved in this planning are usually obtained by manually measuring on radiographic images (91.44 cm cassette for alignment film in weight bearing stance). We have devised a system which makes it possible to automate the measurements. It automatically finds the cortical bone internal and external contours from full femur and tibia. Detection of bone boundaries is achieved using active contours. The snake is initialized with the interactive definition of a poligonal contour on the radiographic image. From the obtained contours, the parameters can be easily derived. The system speeds up the measuring processes and eliminates subjectivity.

Keywords: medical images, active contours, orthopaedics, total knee replacement (TKR).

Introduction

Total knee replacement (TKR) is a surgical procedure of the treatment of degenerative ostheoarthritis of the knee, reumathoid arthritis, or in processes that lead to an unrecoverable damage of the knee joint. This technique requires an adequate planning, including among others the following aspects: morphological measurements of the joint to be replaced, measurements of parameters in order to achieve a good alignment and prosthesis fitting, and even 3D reconstruction of the bone geometry in the case of great bone defects. Several parameters involved in the surgical planning (Bargren et al., 1983) are shown in Fig. 1: distal femur width (DFW), tibial plateau width (TPW), distal femoral shaft diameter (DFSD), proximal femoral shaft diameter (PFSD), tibiofemoral angle (TF), capitomidcondylar tibial shaft angle (CMTS) and tibial plateau tibial shaft angle (TPTS). The values of DFW and TPW are directly obtained from

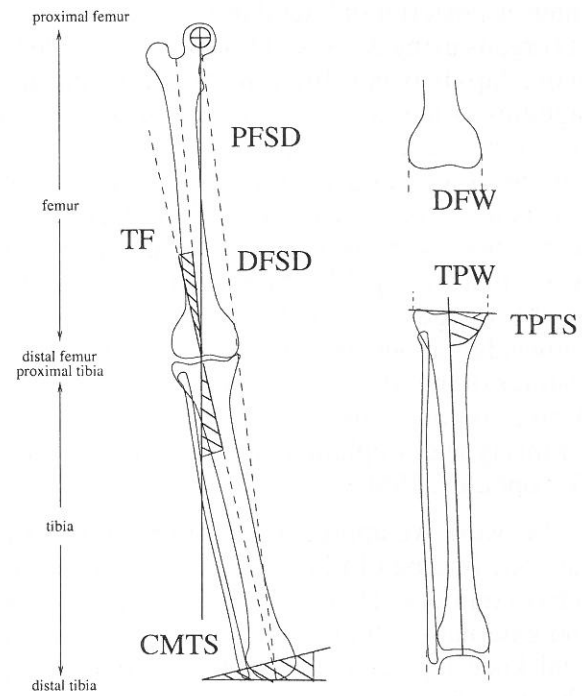

Fig. 1. Outline of the distances and angles involved in total knee arthroplasty: distal femur width (DFW), tibial plateau width (TPW), distal femoral shaft diameter (DFSD), proximal femoral shaft diameter (PFSD), tibiofemoral angle (TF), capitomiocondylar tibial shaft angle (CMTS) and tibial plateau tibial shaft angle (TPTS).

* This work was supported by Xunta de Galicia under Grant XUGA20603B96

the external contour of the cortical bone of the femur and tibia in the knee joint. The values of DFSD and PFSD are obtained from the axial length of the femur. These values are calculated as the width of the femur at fixed relative positions on the femur. The TF value is the angle between the symmetry axis of tibia and femur (anatomic alignment). The CMTS value is the angle between the axis capitomiocondylar and the symmetry axis of the tibia (mechanical alignment) as shown in Fig. 1. Finally, the angle between the tibial plateau and the symmetry axis of the tibia gives us the value of TPTS.

These measurements are performed on radiographic images of different projections of the knee joint (Bargren et al., 1983; Moreland, 1988). The correct segmentation of the cortical bone in the tibia and femur, and the definition of the symmetry axis would allow us to make measurements automatically. Unfortunately, radiographic images present severe drawbacks for segmentation processes. Among others, we must point out the low signal-to-noise ratio and the fact that these 2D images are obtained as anterior-posterior or lateral projection images of 3D organs using X-rays. This leads to problems of overlaps between different structures and ambiguities, since a small volume of a strongly absorbing material can produce the same pixel grey level as a larger volume of a more X-ray transparent tissue. Because of these facts, it becomes necessary to employ segmentation processes that are capable of integrating constraints on the image data together with the a priori knowledge about the location, size, shape and features of the structures of interest in the scene. Active contours provide an appropriate scheme for this type of implementation (McInerney and Terzopoulos, 1996).

In this work we approach the problem of cortical bone finding of tibia and femur by means of active contours. Then, the cortical bone internal and external contours of the bones involved in total knee replacement (TKR) are delineated. These contours will permit the automatic estimation of the parameters required in the surgical planning of TKR. The latter takes advantage of this and extra information such as: 3D reconstruction of bones from computed tomography (CT) scans, injury labelling and knowledge about stress distribution in the knee joint. All these aspects are being treated in order to provide the surgeon with a semiautomatic system to support surgical planning. This paper is about only one of the aspects that made up the global project.

The work is structured into the following sections: first we introduce the background theory of snakes; then we describe the procedures to find the outer and inner contours of the cortical bone, as well as the benefits of new energy terms; and finally, we present the results and main conclusions of this work.

Deformable Models: Snakes

A snake (Kass et al., 1988) is an elastic curve that, located over an image, evolves from its initial shape and position as a result of the combined action of external and internal forces. External forces lead the snake towards the features of the image, whereas internal forces model the elasticity of the curve. The snake is defined by constructing a suitable deformation energy. In a parametric representation, the snake appears as a curve $u(s) = (x(s), y(s)), s \in [0, 1]$, with $u(0) = u(1)$. Its internal energy is

$$E_{int}(u(s)) = \alpha|u_s(s)|^2 + \beta|u_{ss}(s)|^2. \quad (1)$$

It is made up of two factors: the membrane energy $\alpha|u_s(s)|^2$, which weights its resistance to stretching, and the thin-plate energy $\beta|u_{ss}(s)|^2$, that weights its resistance to bending. $u_s(s)$ and $u_{ss}(s)$ represent the first and second derivatives respectively. The elasticity parameters α and β control the smoothness of the curve.
The external energy is generally defined as a potential field P,

$$E_{ext}(u) = \int_0^1 P(u(s))ds. \quad (2)$$

The external energy *pushes* the snake towards the features of the image that are being seeked for. Typical terms in the expression of the external energy are (Cohen and Cohen, 1993, Radeva and Serrat, 1995): $P_I = \pm\gamma I(u(s))$, where $I(x, y)$ is the intensity image, and attracts the curve to high (or low) intensity points; $P_G = -\zeta|\nabla(G_\sigma(u(s)) * I(u(s)))|$, where G_σ represents a Gaussian filter with scale parameter σ, and attracts the curve to intensity edges, after convolution with a Gaussian smoothing;

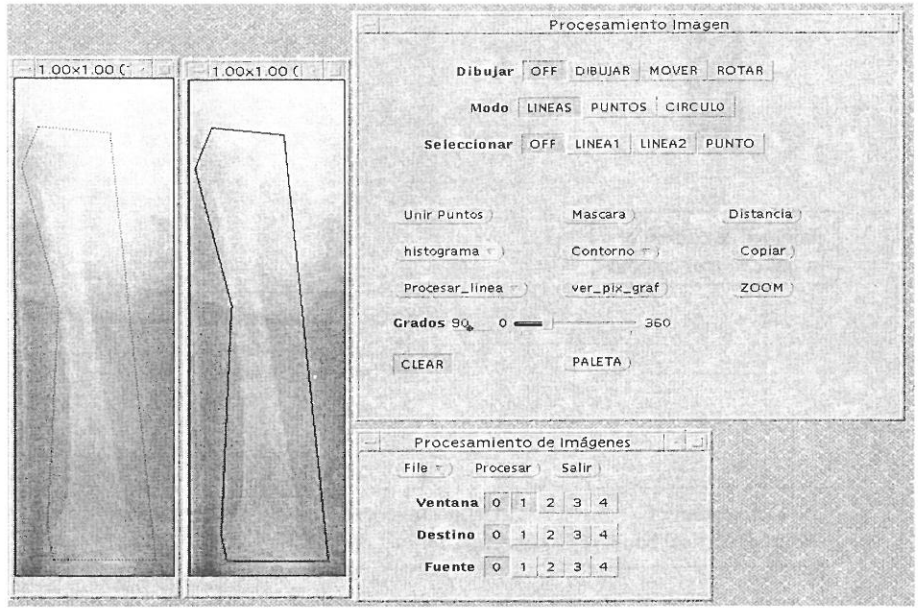

Fig. 2. Interactive drawing of initial contour.

and $P_E = -\eta e^{-d(u(s))^2}$, where $d(u(s))$ is the distance to the closest boundary point, which pushes the contour to the edge points of an edge map. An edge map is an image of contours detected by means of an edge detector filter. γ, η, ζ are positive constants that weight the contributions of the different terms in the external energy. The total energy of the snake will be the sum of the external and internal energies along the curve $u(s)$:

$$E_{snake} = \int [E_{int}(u(s)) + E_{ext}(u(s))]ds \quad (3)$$

The dynamic minimization of this functional *pushes* the snake to the features of interest, depending on the application.

In order to numerically compute a minimal energy solution, it is necessary to discretize the energy E_{snake}. A general approach to discretization of energies is to aproximate the function of interest u as a set of linear superposition of basis functions weighted by nodal variables u_i. In our case, u will be represented by spline aproximations, and the set u_i, $i = 1, \ldots, n$ will be a set of points that define the guiding polygon.

Procedures

Our system is applied to radiographic images of the tibia and femur. The system starts with the user interactive edition of a set of vertices using a graphical environment as shown in Fig. 2. From this set of vertices, a polygonal contour is defined. Then, this initial contour automatically evolves, under control of internal and external forces, until it delineates, first the external contour of the cortical bone of the femur, and finally its internal contour. From these contours, we can automatically obtain a set of parameters needed for the surgical planning of the knee replacement. A flow chart of the system is shown in Fig. 3.

Obtaining the Femur External Contour: New Potential Term

The system for obtaining the external contour of cortical bone is based on snakes. The process begins with manual selection of a set of n vertex in the 2D radiographic image. A number n about 10 points is enough. This set defines an initial polygonal approximation of the contour. Then the system selects N points evenly spaced over the polygonal approximation in a ratio of 1 to 4. This discretized contour, made up of N points (snaxels), will evolve attracted by the local minima of the external potentials and under the constraints imposed by internal forces. When the total energy of the snake reaches its minimun value the deformation stops. Here, we

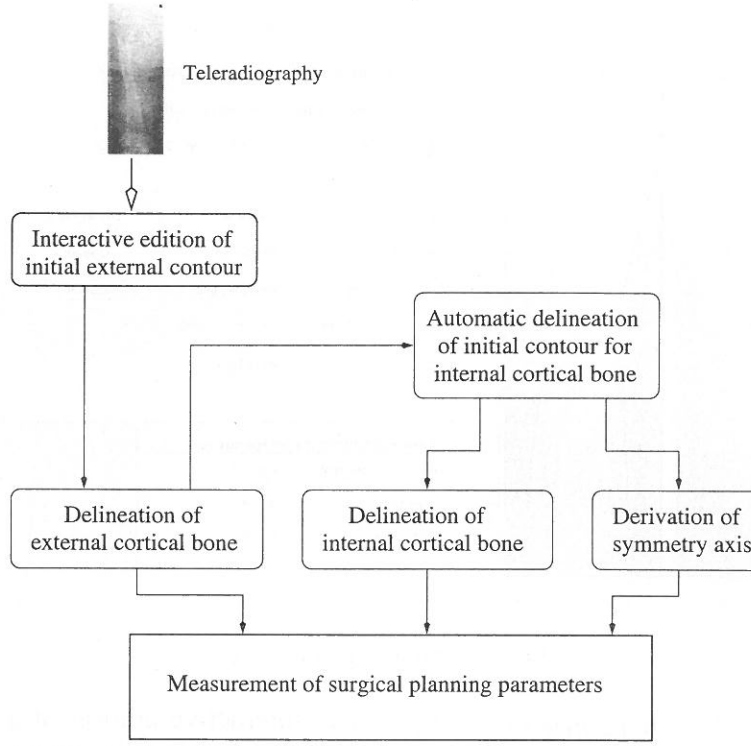

Fig. 3. Scheme of the system.

adopt for the internal energy the classical form, whose discrete version is:

$$E_{int}(u) = \sum_{i=1}^{N} \alpha \frac{|u_i - u_{i-1}|^2}{2} + \beta \frac{|u_{i-1} - 2u_i + u_{i+1}|^2}{2}, \quad (4)$$

where N represents the number of vertex u_i, $i = 1 \ldots, N$. For the external energy we consider the following potential terms

$$E_{ext}(u) = \sum_{i=0}^{N} -\zeta |\nabla (G_\sigma(u_i) * I(u_i))| - \eta log_a(1 + d(u_i)) - \nu C(u_i), \quad (5)$$

where ζ, η, ν are positive constants, $d(u_i)$ represents the euclidean distance from point u_i to the nearest edge point and base a introduces high level information about what is understood as points that are close and points that are far from the nearest edge point (Radeva et al., 1995). We make use of edge points extracted by a Canny filter (1986) prior to the use of the active contour. The first two terms are classical ones, and the last term, C, is a new energy term that is specifically introduced for our problem. The first term refers to the gradient, the second one to the distance from each vertex of the snake to the closest edge point in an edge map, and the third one eliminates the ambiguity that appears when the snake is located between the boundaries of two neighboring structures. This term will attract the snake towards the contour of the structure that it encloses, and will push away the snake from other structures. With this formulation, the snake will be attracted by strong intensity edges in the external side of the cortical bone.

If the initialization is not good enough and we only consider the first two terms of the external energy, the snake could get trapped by edge points of the nearby structures. This may happen in the joints. In Fig. 4a we represent the case of two very close objects and an inaccurate initial position of the snake over the proximal part of the tibia. In this situation, the first two terms of the potential cannot distinguish between the edges of the tibia and the femur, and thus the snake would fit on the closest one, as can be seen in Fig. 4b. To fit the contour to the external cortical bone of the femur, term $C(u(s))$ is introduced. This new energy term carries out information regarding the contrast between two regions on both sides of the snake. It has the

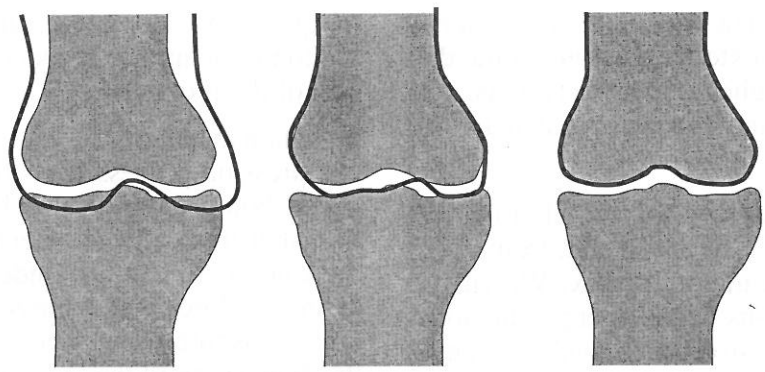

Fig. 4. Effect of region information.

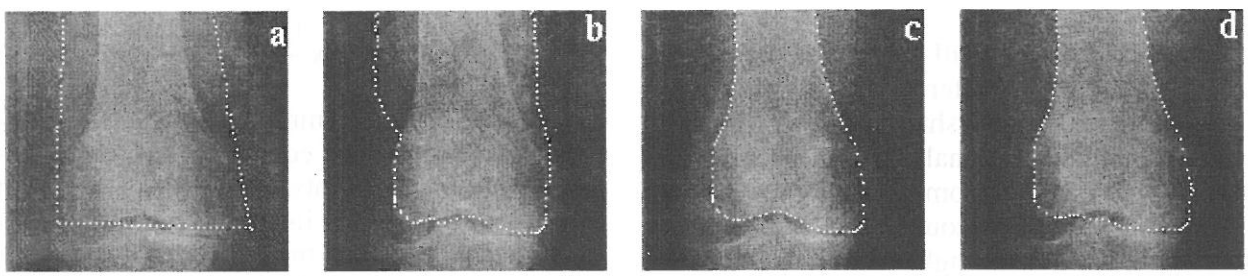

Fig. 5. Evolution of the initial contour towards external edges of the distal femur: (a) initial contour, (b) intermediate contour and (c) final contour with the new internal energy term C, (d) result obtained with classical energy terms (without C).

following expression:

$$C(u_i) = \frac{|F_i^{int} - F_i^{ext}|}{F_i^{int} - F_i^{ext}} \tag{6}$$

with

$$F_i^{int} = \frac{1}{A_i^{int}} \sum_{i \in R_i^{int}} f_i, \quad F_i^{ext} = \frac{1}{A_i^{ext}} \sum_{j \in R_i^{ext}} f_j, \tag{7}$$

where R_i^{int} and R_i^{ext} are two rectangular subregions with a shared edge. This edge will be tangent to the snake and centered on point u_i, so, R_i^{int} will be on the internal side of the snake and R_i^{ext} on the external side. The size of the rectangle is 3×5 pixels, 3 pixels in the tangent direction and 5 pixels in the normal direction to the snake. A represents the size of the region and F represents the average value of some feature in the region. This potential will fit the snake to the edges that present a larger value of the property F towards the inside of the snake. In this implementation F is the average intensity, but any other property could be used. At the end, the result is the one shown in Fig. 4c.

The external contour of the bone is reached as a result of the evolution of the snake from an initial contour. This behavior can be seen with real images in Fig. 5, where we show the behavior of the snake in the distal femur. Fig. 5a is a polygonal approximation manually traced by the user. Once the initial contour has been chosen, it will evolve (Fig. 5b) until it reaches the external contour of the femur as shown in Fig. 5c. In Fig. 5d we show the result reached by means of the classical energy terms, without the effect of the new internal energy term (C) we propose. In this case the snake is trapped in potential wells corresponding to the tibia. As can be seen, the term C improves the classical approach as now the snake can distinguish between tibia and femur.

Obtaining the Femur Internal Contour: New Internal and External Energy Terms

After obtaining the external contour of the cortical bone, the next step is delineation of the bone internal cortex. From the knowledge of the femur height, and using proportionality ratios, the femur is divided into three areas: proximal end, distal end, and shaft. The internal cortex is defined in the shaft, so we only consider this

part of the bone. The height of the femur is calculated from its external contour as the distance between its highest and lowest points. The width of the bone in particular areas may also be obtained.

Two problems have to be solved: (1) to obtain an initial contour for the snake and, from it, (2) to fit the snake to the internal cortex. We will use two new formulations of the energy functional to solve each of the aforementioned problems.

The Initial Contour

The initial contour will be obtained from the delineation of the external cortical bone and the symmetry of the shaft in the formulation of the energy functional will be taken advantage of. To facilitate some calculations, we will reparametrize the contour of the external cortical bone, so that the right and left parts of the contour will have the same number of vertices, evenly spaced along the vertical axis. Thus, each point of the right side will have a corresponding one on the left side with the same vertical coordinate. This way, the search for the vertex symmetric to another one would be faster. We will use an energy minimization algorithm that does not permit vertical displacements of the u_i points of the snake. This does not affect the quality of the solution, but keeps the symmetry condition and so reduces the computational cost of the process.

To obtain the internal cortex, we will carry out a compression process over the external contour of the bone shaft. In this line, the contour is liberated from all the external forces we have indicated before and it undergoes the effect of an inward force in the horizontal direction. The aim of this force is to place the initial contour for the delineation of the internal cortex around the bone symmetry axis. This horizontal compression force leads to the following internal energy term:

$$E_{int}^{comp}(u_i) = \kappa \frac{||u_i - u_{i_s} - \delta||}{DFW}, \qquad (8)$$

where u_i and u_{i_s} are symmetric points, δ is a constant that defines the equilibrium distance between symmetric points, and DFW is the width of the distal femur as ilustrated in Fig. 1. This parameter is obtained from the external contour of the cortical bone as the maximal width in the distal femur.

We add the membrane and the thin-plate energy terms in order to preserve the smoothness of the curve. The evolution of the contour stops around the symmetry axis of the bone once the internal cortex has been surpassed. This fact can be seen in Fig. 6. Fig. 6a shows the contour obtained for the cortical bone. The external

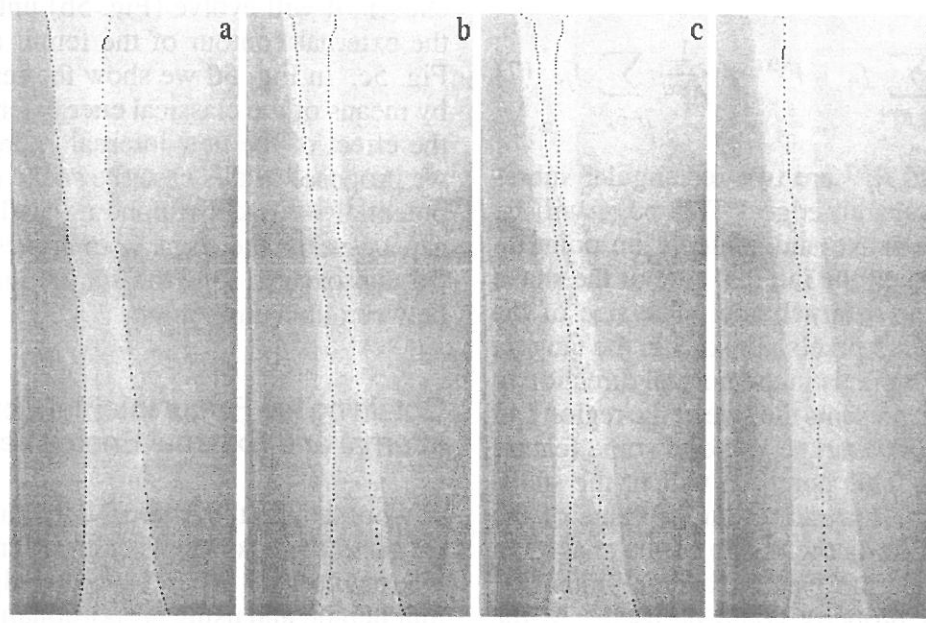

Fig. 6. Evolution of the compression of the sides of the femur and symmetry axis: (a) external contour of the cortical bone, (b) evolution towards the symmetry axis, (c) halt of the evolution of the initial contour for delineation of internal cortex), and (d) obtained symmetry axis.

energy in this case is zero, so the total energy equals the internal energy:

$$E_{int}(u) = \sum_{i=1}^{N} E_{int}^{comp}(u_i) + \alpha \frac{|u_i - u_{i-1}|^2}{2} + \beta \frac{|u_{i-1} - 2u_i + u_{i+1}|^2}{2}. \quad (9)$$

Figs. 6.b-c show an intermediate state and the final position of the contour around the symmetry axis respectively. The symmetry axis $U^{sym}(y)$ (Fig. 6.d) is defined from the set of halfway points between symmetric points of Fig. 6.c.

Delineation of the Internal Contour

Once the contour is located around the bone symmetry axis, its evolution towards the internal cortex starts. The definition of new expressions for the energy functional is now neccesary. From this symmetry axis, we are going to define the internal energy, to simplify the expression of the internal energy, to eliminate the problems associated with adjustments of the elasticity parameters (too much rigidness or not enough robustness with respect to noise) and to introduce

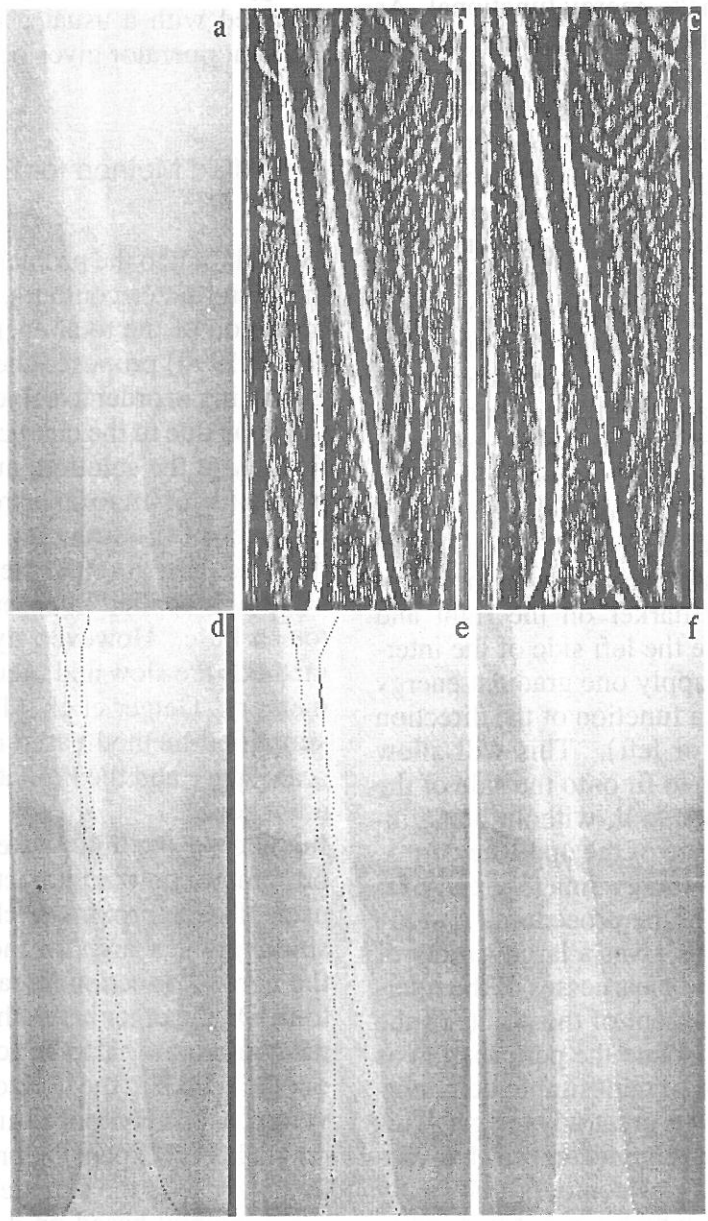

Fig. 7. (a) Original image; energy images: (b) $G_1(x, y)$ and (c) $G_2(x, y)$; (d-e) evolution of the contour towards the internal cortex; (f) bad result obtained with the commonly used filter.

domain knowledge (symmetry) by:

$$E_{int}(u) = c \sum_i |u_i - 2u_i^{sym} + u_{i_s}|, \qquad (10)$$

where c is a positive constant and u_{i_s} is the point of the deformable contour symmetrically located with respect to u_i. For each point $u_i = (x_i, y_i)$, the corresponding point of the symmetry axis will be $u_i^{sym} = U^{sym}(y_i)$. $U^{sym}(y)$ is the symmetry axis previously obtained. The internal energy minimum corresponds to the case of symmetry with respect to the central axis of the internal contours of the bone.

In order to better adapt to the new conditions, we reformulate the snake energy functional. As the internal cortex of the femur presents a longitudinal disposition of the trabecula, a filter that is sensitive to this circumstance would optimize the energy term (compare Figs. 7.e and 7.f). In this case we employ a filter that provides a measure of the gradient only in the horizontal direction. Two potential images are generated, Figs. 7.b-c, one obtained by the maximum between 0 and the difference between the value of the pixel and its neighbor to the left, $G_1(x, y) = \max\{0, I(x, y) - I(x-1, y)\}$ and the other by the maximum between 0 and the difference between the value of the pixel and its neighbor to the right, $G_2(x, y) = \max\{0, I(x, y) - I(x+1, y)\}$. In one, dark contour on the left and lighter contours on the right will be found, among them the right side of the internal cortex. In the other, the contours will be darker on the right and lighter on the left, like the left side of the internal cortex. Now, we apply one gradient energy image or the other as a function of the direction of the normal (right or left). This will allow each side of the snake to fit onto the side of the cortex that corresponds to it, without being influenced by the presence of the opposite cortex. This duplicity of the energy image greatly facilitates carrying out of the procedure. A study over femur radiographs gives a large variety of thicknesses, depths and clearnesses of the internal cortex. Local treatment of the points of the snake, which tend to isolate the perturbation as much as possible, due to undesirable neighboring structures, implies a great advantage. This is not only in the convergence speed, but also in the production of final contours that really define the cortex and which are not trapped in potential wells that are a consequence of the interferences we mentioned before.

In order to further accelerate the convergence process, we use, as a second term of the potential, the distance to edge points.

$$E_{ext}(u) = \sum_{i=1}^{N} -\bar{\zeta} G_{1,2}(u_i) - \bar{\eta} log_a(1 + d(u_i)), \qquad (11)$$

where $\bar{\zeta}$ and $\bar{\eta}$ are constants again. The minimization of this energy functional will be the last step in order to make the deformable model smoothly adapt to the internal cortex. Figs. 7d-e show an intermediate state and the location of the internal contour of the cortical bone for the energy minimum. In Fig. 7f we show the result obtained with a usual gradient operator. Our gradient operator gives better results.

Simplified Method for Energy Minimization

The solution to the problem, the detection of the inner and outer contours, is given by the minimization of the total energy functions. Amini et al. (1990) proposed the use of dynamic programming in order to solve variational problems in vision due to the characteristics of global optimality of the solution, numerical stability and possibility of imposing strong constraints on the behavior of the structure. Their algorithm was iterative, and in each step dynamic programming was applied in order to improve the contour a little. However, dynamic programming methods are slow and require a large amount of memory. Geiger et al. (1995) propose a more simplified method based on the analysis of the scale space and the limitation of the snake variation zone.

In our case, the initial external contour is an approximate contour interactively provided by the user. This approximate character permits constraining the search for the energy minimum in the normal direction to each vertex of the contour. On the other hand, the search for the internal contour may also be accelerated by carrying out the search in the horizontal direction to each vertex, as the contour fitting process consists of only a lateral expansion process from a position that is close to the symmetry axis. As such, we use a method based on dynamic programming where a segment of the possible displacement of the snake vertices is defined for each vertex

of the snake. Each segment is centred on a vertex and is parallel to the horizontal axis. In this way, without worsening the solution, computation times achieved that are 10 times lower than were those when all the neighborhood had to be explored. A more detailed description of the minimization algorithm can be found in Pardo et al. (1997).

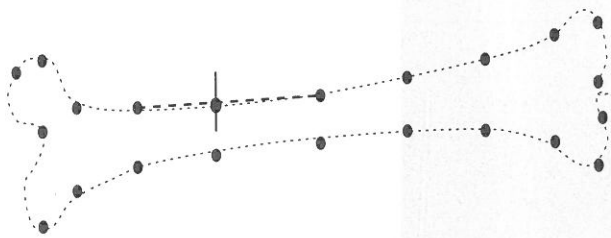

Fig. 8. Segments of a possible variation of the snake.

Given three consecutive control points (vertices) u_k, u_{k+1}, u_{k+2}, the vertex u_{k+1} was only able to move perpendicular to the straight line connecting u_k and u_{k+2} as indicated in Fig. 8. These segments, inside which a variation is allowed, are centred on each of the control points. After this, starting from an arbitrary vertex, initially taken as fixed, dynamic programming to determine the position of the remaining control points of the contour for the energy minimum was used. The starting vertex changes in each iteration of the algorithm, then the constraint of going through the fixed initial and final points is eliminated. The process is repeated until a global energy minimum of the snake is achieved. In each iteration the segment of the control points variation is recalculated to flexibilize the shape of the snake. The segment is determined from the normal to the curve for the external contour of the cortical bone, and parallel to the horizontal axis for the internal contour. The process is very fast and achieves good results.

Results and Conclusions

Our system allows automatic delineation of bones internal and external contours from radiographic images of full femur and tibia. The process starts after an initial contour is provided by interactively selecting a set of points that define an approximate polygonal contour all around the bone. From the final result (inner and outer contours, and symmetry axis) the calculations of the aforementioned parameters may be implemented for their automatic execution.

In Figs. 9 and 10 the results obtained on the teleradiography of another patient are shown. The user interactively supplies an initial contour as in Fig. 9.a and Fig. 10.a. Our system does not need precise initialisation. Fig. 9.b contains the external contour of the cortical bone. From this contour, as we have described before,

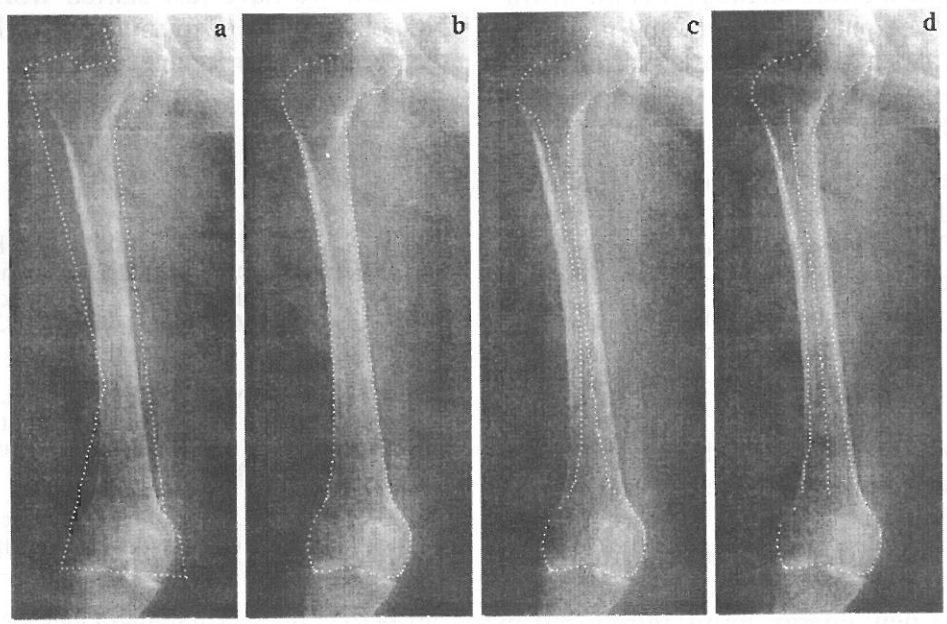

Fig. 9. (a) Initial contour for the external contour; (b) external contour(c); (d) initial contour for the internal cortour; (f) internal contour and symmetry axis.

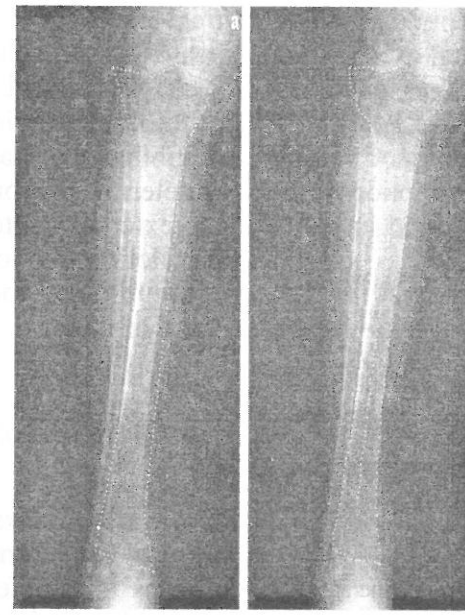

Fig. 10. (a) Initial contour for the external contour; (b) external contour of the tibia and symmetry axis.

the initial contour for the detection of the internal cortical bone is automatically obtained (Fig. 9.c). Fig. 9.d shows the internal contour of the cortical bone and the symmetry axis. Finally, Fig. 10.b contains the delineation of the external cortical bone from tibia.

There are several advantages provided by this automatic method with respect to the manual one. It frees the specialist from the tedious labour of tracing lines and angles manually in order to calculate the parameters. It prevents all the measurement errors on the part of the instruments employed, such as rulers and goniometers. It provides a semiautomatic platform that reduces the specialists work to the simple introduction of the initial contour.

Summarizing, the use of active contours in the field of total knee replacement permits the automation of processes that facilitate the work of specialists and minimize the number of errors. Their simplicity, intuitiveness and versatility provided by the possibility of injecting domain knowledge in the form of energy functions, make active contours especially adequate for this type of tasks. The deformable models we propose implement new definitions of internal and external energies that solve problems which affect the segmentation of X-ray images of bones in the classical formulation of snakes. The new energy terms introduced in our formulation improve the results obtained by the classical one. Our scheme does not need a good initial approximation, which would be mandatory with the classical snake model.

The image data are acquired for live subjects, and thus true (ideal) segmentation cannot be established. Therefore, we decided to assess accuracy of the method by visual inspection of the results obtained from different cases. These results, checked up by surgeons, validate the method. Moreover, the algorithm is very fast (it takes a few seconds) and repeatable (it does not need a very accurate intial contour). At the moment we have just started working on the part of the system for automatically obtaining the parameters from the contours.

References

[1] A. A. Amini, T. E. Weymouth and R. C. Jain Using dynamic programming for solving variational problems in vision. IEEE Transactions on Pattern Analysis and Machine Intelligence, 12 (1990), 855–867.

[2] J. H. Bargren, J. D. Blha and M. A. Freeman Alignment in total knee arthroplasty: correlated biomechanical and clinical observations. Clinic Orthopaedic (1983), 173–178.

[3] J. Canny A computational approach to edge detection. IEEE Transactions on Pattern Analysis and Machine Intelligence, 8 (1986), 679–698.

[4] L. D. Cohen and I. Cohen Finite-element methods for active contour models and balloons for 2–D and 3–D images. IEEE Transactions on Pattern Analysis and Machine Intelligence, 11 (1993), 1131–1147.

[5] D. GEIGER, A. GUPTA, L. A. COSTA AND J. VLONTZOS Dynamic programing for detecting, tracking, and matching deformable contours. IEEE Transactions on Pattern Analysis and Machine Intelligence, 17 (1995), 294–302.

[6] M. KASS, A. WITKIN AND D. TERZOPOULOS Snake: active contour models. International Journal of Computer Vision, 1(1988), 321–331.

[7] T. MCINERNEY AND D. TERZOPOULOS Deformable models in medical image analysis: a survey. Medical Image Analysis, 1 (1996), 91–108.

[8] J. R. MORELAND Mechanisms of failure in total knee arthroplasty. Clinic Orthopaedic (1988), 226–249.

[9] J. M. PARDO AND D. CABELLO AND J. HERAS A snake for model-based segmentation of biomedial images. Pattern Recognition Letters, 18 (1997), 1529–1538.

[10] P. RADEVA, J. SERRAT AND E. MARTI A Snake for model-based segmentation. Proceedings of International Conference on Computer Vision, (1995) MIT, USA.

Received: May, 1997
Revised: February, 1998
Accepted: April, 1998

Contact address:
J. M. Pardo, F. Vilariño, M. J. Carreira,
Dpto. Electrónica e Computación
Facultade de Física
Universidade de Santiago de Compostela
Campus Sur,
15706 Santiago de Compostela
A Coruña
fax: +34 81 599412
e-mail: {pardo,fernando}@dec.usc.es
Spain

JOSE M. PARDO was born in 1968 in Malpica (A Coruna), Spain. He recived the B.Sc. and de Ph.D. degrees in Physics in 1991 and 1998, respectively, from the University of Santiago de Compostela. Since November 1993 he has been an assistant professor at the Mathmatics and Physics Faculties of the University of Santiago de Compostela where he is teaching undergraduate courses related to computer science and digital image processing. His current research interest is medical image analysis, including stochastic labeling, segmentation by deformable models and solid modeling.

FERNANDO L. VILARIÑO recived the B.Sc. and the M.Sc. degrees in Physics from the University of Santiago de Compostela, Spain, in 1996 and 1997 respectively. Currently, he is a Ph.D. student at the Department of Electronics and Computer Science. His work is focused on medical image segmentation and the study of shape for 3D reconstruction.

MARIA J. CARREIRA received the B.Sc. and Ph.D. degrees in Physics from the University of Santiago de Compostela, Spain, in 1989 and 1996, respectively. Since 1991 she has been an assistant professor of computer science in the University of Santiago de Compostela, Spain. Her current research interests include computer vision, pattern recognition, biomedical image processing and perceptual grouping.

RAMON TURNES recived the B.Sc. and the M.Sc. degrees in Physics from the University of Santiago de Compostela, Spain, in 1993 and 1995 respectively. Currently, he is a Ph.D. student at the Department of Electronics and Computer Science. His current research interests include computer vision and perceptual grouping.

DIEGO CABELLO received the Ph.D. degree in Physics from the University of Santiago de Compostela in 1984. Present appointment: professor of electronics and dean of the Faculty of Physics of the University of Santiago de Compostela. His research interest is in microelectronic implemetation of artificial neural networks for early vision, and developtment of intelligent systems for image understanding.

JOAQUÍN HERAS was born in 1954 and received the B.Sc. degree in Medicine from the University of Salamanca, Spain in 1979. Present appointment: staff member and predoctoral research in the Orthopaedic Surgery and Trauma Dpt. of the General Hospital of the University of Santiago de Compostela. His research interest and lines are: artificial intelligence and expert systems development in total joint replacement domain, artificial neural networks (applications in CT and radiographic image analysis) and biomaterials and bone-tissue interactions. Clinical special interest in joint reconstruction.

JOSÉ COUCEIRO was born in 1939 and received the B.Sc. degree in Medicine from the University of Santiago de Compostela, Spain in 1963. He received the Ph.D. degree in medicine from the University of Santiago de Compostela, Spain, in 1980. Present appointment: Professor and chief of the Orthopaedic Surgery and Trauma Dpt. of the General Hospital of the University of Santiago de Compostela, Spain and his research special interest is in joint reconstruction and autologous chondrocyte implantation. Professor Couceiro is O.Fellow of the British Orthopaedic Association and the Girdlestone Orthopaedic Society.